An Analytical Framework for Performance Evaluation of IPv6-Based Mobility Management Protocols

Christian Makaya, *Student Member, IEEE,* and Samuel Pierre, *Senior Member, IEEE*

***Abstract*— Mobility management with provision of seamless handover is crucial for an efficient support of global roaming of mobile nodes (MNs) in next-generation wireless networks (NGWN). Mobile IPv6 (MIPv6) and its extensions were proposed by IETF for IP layer mobility management. However, performance of IPv6-based mobility management schemes is highly dependent on traffic characteristics and user mobility models. Consequently, it is important to assess this performance in-depth through those two factors. The performance of IPv6-based mobility management schemes is usually evaluated through simulations. This paper proposes an analytical framework to evaluate the performance of IPv6-based mobility management protocols. This proposal does not aim to advocate which is better but rather to study the effects of various network parameters on the performance of these protocols to enlighten decision-making. The effect of system parameters, such as subnet residence time, packet arrival rate and wireless link delay, is investigated for performance evaluation with respect to various metrics like signaling overhead cost, handoff latency and packet loss. Numerical results show that there is a trade-off between performance metrics and network parameters.**

***Index Terms*— Analytical modeling, IP mobility protocols, mobility management, performance evaluation, quality of service, wireless networks.**

I. Introduction

NEXT-generation wireless networks (NGWN) or fourth generation wireless networks (4G) are expected to exhibit heterogeneity in terms of wireless access technologies and services. With NGWN/4G, mobile nodes (MNs) or subscribers will have more demands for seamless roaming across different wireless networks, support of various services (e.g., multimedia applications) and quality of service (QoS) guarantees. Conceptually, the NGWN architecture can be viewed as many overlapping wireless access domains (e.g., UMTS, CDMA2000, WLAN, WiMAX). However, this heterogeneity brings new challenges for architecture design, mobility management, QoS provision and security. Moreover, heterogeneity in terms of radio access technologies and network protocols in NGWN requires common interconnection elements. Since the Internet Protocol (IP) technology enables the support of applications in a cost effective and scalable way, it is expected to become the core backbone network of NGWN [1]. Thus, current trends in communication networks evolution are directed towards all-IP principles in order to hide the heterogeneity and achieve convergence of these various networks.

Mobility management with provision of seamless handoff is key topic in NGWN/4G. Then, it is crucial to provide seamless mobility and service continuity in intelligent and efficient ways. The Internet Engineering Task Force (IETF) has proposed Mobile IPv6 (MIPv6) [2] as the main protocol for mobility management at the IP layer. However, MIPv6 has some well known drawbacks such as signaling traffic overhead, especially when the home agent (HA) or the correspondent node (CN) is located geographically far away from the mobile node (MN). Message transmission time for binding update registration will become very high resulting in long delay (handoff latency) and high packet loss rate thereby causing user-perceptible deterioration of real-time traffic.

Then, several extensions such as Fast Handovers for MIPv6 (FMIPv6) [3] and Hierarchical MIPv6 (HMIPv6) [4], have been proposed to enhance MIPv6 performance. In spite of these extensions, mobility management with QoS provision in NGWN remains a challenging and complex task. Usually, performance evaluation of IP-based mobility management schemes is based on simulation and testbed approaches and most available work focuses on these aspects [5], [6]. However, scenarios used for simulations vary greatly, the comparison of IP-based handoff protocols is hardly possible. Few works are available in the literature which assess IPv6-based mobility management protocols through analytical models. On the other hand, they are often based on simple assumptions and have some drawbacks.

In [7], trade-off relationship between location update cost and packet tunneling cost is introduced in order to compute total signaling cost and evaluate the efficiency of IP-based mobility protocols. Work presented in [7] is largely based on concepts introduced for location management in personal communication systems (PCS). Analytical models for handoff latency of IPv6-based mobility protocols are presented in [8] in order to assess the most appropriate scheme for functional specification and implementation. Analysis of signaling bandwidth according to binding update emission frequency is presented in [9]. However, signaling overhead generated by packet tunneling is not considered. An analytical

Manuscript received September 22, 2006; revised November 27, 2006 and January 22, 2007; accepted March 7, 2007. The associate editor coordinating the review of this paper and approving it for publication was Y.-B. Lin. This work was supported in part by the NSERC-Ericsson Industrial Chair.

The authors are with the Mobile Computing and Networking Research Laboratory (LARIM), Department of Computer Engineering, Ecole Polytechnique de Montreal, P.O. Box 6079, Station Centre-ville, Montreal, Quebec, H3C 3A7, Canada (e-mail: {christian.makaya, samuel.pierre}@polymtl.ca).

Digital Object Identifier 10.1109/TWC.2008.060725.

model for performance evaluation of HMIPv6 in IP-based cellular networks was proposed in [10]. This model ignores periodic binding refresh and binding lifetime period, which may significantly affect total signaling cost. Moreover, the packet delivery cost only takes bandwidth consumption into account for data and ignores the extra signaling consumption due to control traffic. An analysis of the FMIPv6 signaling overhead is compared to that of MIPv6 in [11]. However, packet loss, handoff latency and the impact of user mobility models were not investigated.

Contrary to previous works, in this paper, we perform a comprehensive analysis of various IPv6-based mobility protocols proposed by IETF. We derive signaling overhead cost, packet delivery cost, binding refresh cost and total signaling cost generated by an MN during its subnet residence time for each protocol. Moreover, the required buffer space, handoff latency and packet loss expressions are derived. The effect of mobility and traffic parameters on these criteria are analyzed from numerical results. The remainder of this paper is organized as follows: the next section offers a brief overview of IPv6-based mobility management schemes. After that, the proposed analytical framework is presented. Numerical results based on this analytical model is then investigated before concluding remarks drawn in the last section.

II. IP-BASED MOBILITY MANAGEMENT PROTOCOLS

Mobility management enables systems to locate roaming users in order to deliver data packets, i.e., *location management* and maintain connections with them when moving into a new subnet, i.e., *handover management*. Several protocols have been proposed for these purposes for IP mobility and are briefly presented in this section.

Definition: A *handover* or *handoff* is a movement of an MN between two attachment points, i.e., the process of terminating existing connectivity and obtaining new connectivity. Handovers in IP-based NGWN may involve changes of the access point at the link layer and routing changes at the IP layer.

Efficient mechanisms must ensure seamless handover, i.e., with minimal signaling overhead, handoff latency, packet loss, and handoff failure and service continuity.

Definition: The *handoff latency* at an MN side is the time interval during which an MN cannot send or receive any packets during handoff and it is composed of L2 (link layer) and L3 (IP layer) handoff latencies. The L3 handoff latency is the sum of delay due to: movement detection, IP addresses configuration and binding update procedure.

Definition: The *signaling traffic overhead* is defined as the total number of control packets exchanged between an MN and a mobility agent (e.g., home agent).

A. Mobile IPv6 (MIPv6) [2]

MIPv6 was proposed for mobility management at the IP layer and allows an MN to remain reachable despite its movement within the IP environment. Each MN is always identified by its home address (HoA). While away from its home network, an MN is also associated with a care-of address (CoA), which provides information about the MN's current location. Discovery of new access router (NAR) is performed through Router Solicitation/Advertisement (RS/RA) messages exchange. Furthermore, to ensure that a configured CoA (through stateless or stateful mode [12]) is likely to be unique on the new link, the Duplicate Address Detection (DAD) procedure is performed by exchanging Neighbor Solicitation/Advertisement (NS/NA) messages. After acquiring a CoA, an MN performs binding update to the home agent (HA) through binding update (BU) and binding acknowledgment (BAck) messages exchange. To enable route optimization, BU procedure is also performed to all active CNs.

However, return routability (RR) procedure must be performed before executing a binding update process at CN in order to insure that BU message is authentic and does not originate from a malicious MN. The return routability procedure is based on home address test, i.e., Home Test Init (HoTI) and Home Test (HoT) messages exchange, and care-of address test, i.e., exchange of Care-of Test Init (CoTI) and Care-of Test (CoT) messages. Although RR procedure helps to avoid session hijacking, it increases delay of the BU procedure. Fig. 1(a) represents the sequence of message flow used in MIPv6 based on stateless address autoconfiguration.

Analysis of MIPv6 shows that it has some well-known disadvantages such as overhead of signaling traffic, high packet loss rate and handoff latency, thereby causing user-perceptible deterioration of real-time traffic. Furthermore, the scalability problems arise with MIPv6 since it handles MN local mobility in the same way as global mobility. Simultaneous mobility is another problem MIPv6 faces due to route optimization, which can occur when two communicating MNs have ongoing session and they both move simultaneously [13]. These weaknesses have led to the investigation of other solutions to enhance MIPv6 performance.

B. Fast Handovers for Mobile IPv6 (FMIPv6) [3]

FMIPv6 was proposed to reduce handoff latency and minimize service disruption during handovers pertaining to MIPv6. The link layer information (L2 trigger) is used either to predict or rapidly respond to handover events. When an MN detects its movement toward NAR, by using L2 trigger, it exchanges Router Solicitation for Proxy (RtSolPr) and Proxy Router Advertisement (PrRtAdv) messages with the previous access router (PAR) in order to obtain information about NAR and to configure a new CoA (NCoA). Then, the MN sends a Fast Binding Update (FBU) to PAR in order to associate previous CoA (PCoA) with NCoA. A bi-directional tunnel between PAR and NAR is established to prevent routing failure with Handover Initiate (HI) and Handover Acknowledgment (HAck) message exchanges.

The Fast Binding Acknowledgment (FBAck) message is used to report status about validation of pre-configured NCoA and tunnel establishment to MN. Moreover, the PAR establishes a binding between PCoA and NCoA and tunnels any packets addressed to PCoA towards NCoA through NAR's link. The NAR buffers these forwarded packets until the MN attaches to NAR's link. The MN announces its presence on the new link by sending Router Solicitation (RS) message with the Fast Neighbor Advertisement (FNA) option to NAR. Then,

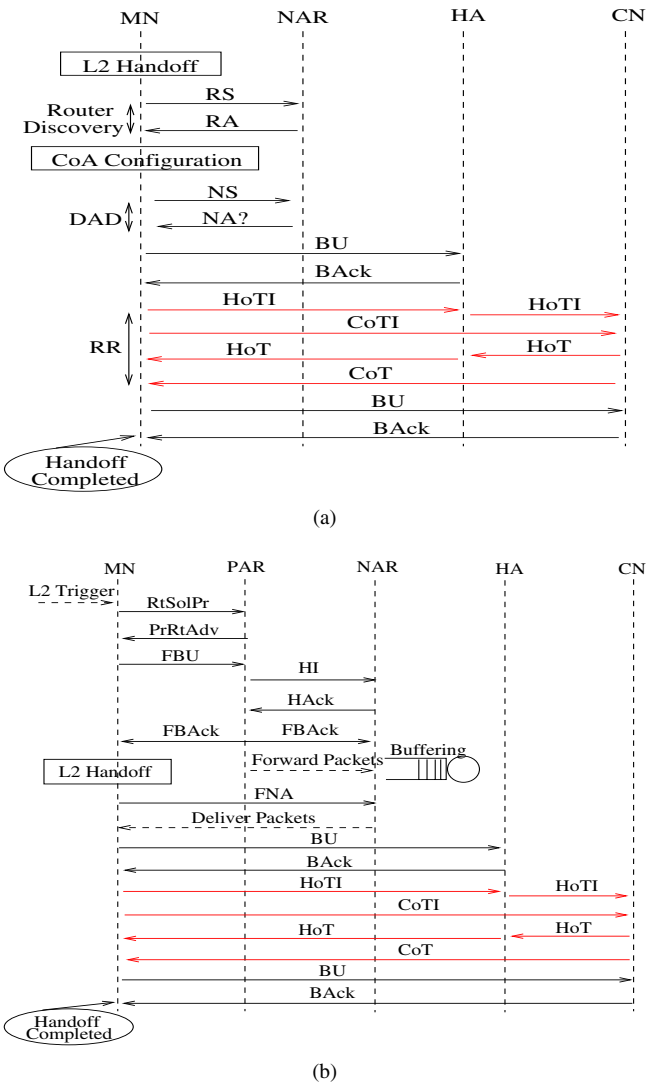

Fig. 1. Signaling messages sequence: (a) MIPv6; (b) FMIPv6.

NAR delivers the buffered packets to the MN. The sequence of messages used in FMIPv6 is illustrated in Fig. 1(b) for MN-initiated handoff of predictive mode.

A counterpart to predictive mode of FMIPv6 is reactive mode. This mode refers to the case where the MN does not receive the FBack on the previous link since either the MN did not send the FBU or the MN has left the link after sending the FBU (which itself may be lost), but before receiving a FBack. In the latter case, since an MN cannot ascertain whether PAR has successfully processed the FBU, it forwards a FBU, encapsulated in the FNA, as soon as it attaches to NAR. If NAR detects that NCoA is in use (address collision) when processing the FNA, it must discard the inner FBU packet and send a Router Advertisement (RA) message with the Neighbor Advertisement Acknowledge (NAACK) option in which NAR may include an alternate IP address for the MN to use. Otherwise, NAR forwards FBU to PAR which responds with FBack. At this time, PAR can start tunneling any packets addressed to PCoA towards NCoA through NAR's link. Then, NAR delivers these packets to the MN.

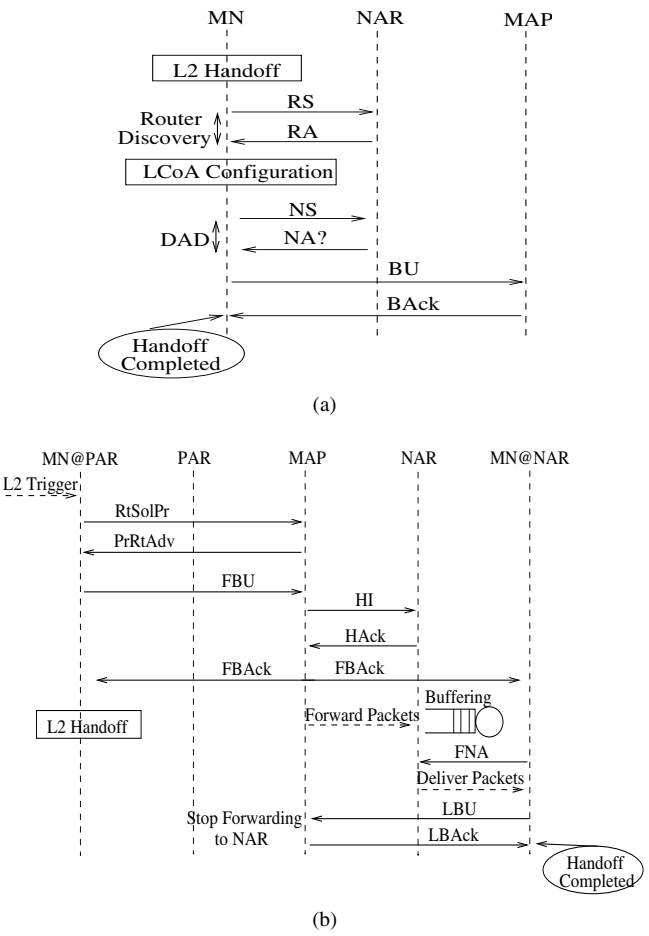

Fig. 2. Signaling messages sequence: (a) HMIPv6; (b) F-HMIPv6.

C. Hierarchical Mobile IPv6 (HMIPv6) [4]

With MIPv6, an MN performs binding update to HA/CNs regardless of its movements to other subnets. This induces unnecessary signaling overhead and latency. To address this problem, HMIPv6 was proposed to handle handoff locally through a special node called Mobility Anchor Point (MAP). The MAP, acting as a local HA in the visited network, will limit the amount of MIPv6 signaling outside its domain and reduce the location update delay. An MN residing in a MAP's domain is configured with two temporary IP addresses: a regional care-of address (RCoA) on the MAP's subnet and an on-link care-of address (LCoA) that corresponds to the current location of the MN.

As long as an MN moves within MAP's domain or access network (AN) it does not need to transmit BU messages to HA/CNs, but only to MAP when its LCoA changes. Hence, the movement of an MN within MAP domain is hidden from HA/CNs. For inter-MAP domain roaming, MIPv6 is used rather than HMIPv6. When an MN crosses a new MAP's domain, moreover from registering with new MAP, BU messages need to be sent by the MN to its HA/CNs to notify them of its new virtual location. Fig. 2(a) presents the generic sequence of message flows used in HMIPv6 with assumption that an MN has entered into new MAP domain and MIPv6 registration procedure was already completed.

D. Fast Handover for HMIPv6 (F-HMIPv6) [14]

Combination of HMIPv6 and FMIPv6 motivates the design of Fast Handover for Hierarchical Mobile IPv6 (F-HMIPv6) protocol [14] in order to allow more efficient network bandwidth usage similarly to HMIPv6. Furthermore, like FMIPv6, it aims to reduce the handoff latency and packet loss. In F-HMIPv6, the bi-directional tunnel is established between MAP and NAR, rather than between PAR and NAR as it is in FMIPv6. After signaling message exchanges (between an MN and the MAP) based on FMIPv6 messages, an MN follows the normal HMIPv6 operations by sending local BU (LBU) to MAP. When MAP receives LBU with the new LCoA (NLCoA) from MN, it will stop packets forwarding to NAR and then clear the established tunnel.

In response to LBU, the MAP sends local BAck (LBAck) to the MN and the remaining procedure follows the operations of HMIPv6. In the original F-HMIPv6 proposal, when handover anticipation cannot be supported, regular operations of HMIPv6 are used [14]. Hence, HMIPv6 corresponds to reactive mode of F-HMIPv6. Fig. 2(b) illustrates a sequence of message used in F-HMIPv6 when an MN moves from PAR to NAR within MAP's domain and the MAP already knows the adequate information on the link-layer address and network prefix of each AR. This illustration is based on the assumption that an MN has entered into a new MAP domain and that MIPv6/HMIPv6 registration procedures were already completed.

III. Analytical Models

In IPv6-based wireless networks, QoS may be defined by packet loss, handoff latency and signaling traffic overhead. Analysis of these metrics is very useful to assess the performance of mobility management protocols in IP-based mobile environments. An analytical framework for evaluating performance of IP mobility protocols is proposed in this section. The notation used in this paper is given in Table I.

Let χ_T be the random variable for the time between L2 trigger generation and link down (i.e., pending L2 handover) and $f_T(u,\sigma)$ the probability density function for successful completion of signaling, where $\sigma > 0$ is a success rate parameter. The probability P_s of anticipated handover signaling success for a particular observed valued t_T is expressed as follows:

$$P_s = Pr(\chi_T > t_T) = \int_{t_T}^{\infty} f_T(u,\sigma)du. \tag{1}$$

Deriving an expression of P_s is difficult, as it depends on the exact form of $f_T(u,\sigma)$, which is usually unknown. For the sake of simplicity, we assume that χ_T is exponentially distributed.

A. User Mobility and Traffic Models

User mobility and traffic models are crucial for efficient system design and performance evaluation. We consider a traffic model composed of two levels, a session and packet. Usually, MN mobility is modeled by the cell residence time and various types of random variables are used for this purpose [18]. In NGWN, although the incoming calls or sessions follow the Poisson process (i.e., inter-arrival time are exponentially distributed), the inter-session arrival times may not be exponentially distributed [18]. Other distribution models, like hyper-Erlang, Gamma and Pareto have been proposed to model various time variables in wireless networks. However, performance evaluations reported in the literature [18] show that exponential model can be appropriate for cost analysis. In fact, exponential model provides an acceptable trade-off between complexity and accuracy.

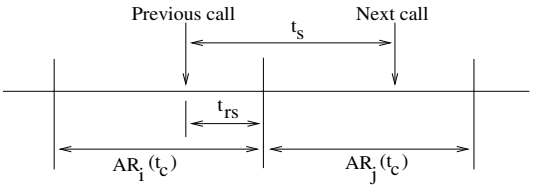

Fig. 3. Timing diagram for subnet boundary crossing.

Let μ_c and μ_d be the border crossing rate of an MN out of a subnet (AR) and out of an access network (AN) or MAP domain, respectively. Furthermore, let μ_l be the border crossing rate for which the MN still stays in the same AN/MAP domain. When an MN crosses an AN/MAP domain border, it also crosses an AR border. Then, according to [16], if we assume that the AN/MAP coverage area is circular with M subnets each with size a_{AR}, the border crossing rates are given by:

$$\mu_d = \frac{\mu_c}{\sqrt{M}} \quad \text{and} \quad \mu_l = \mu_c - \mu_d = \mu_c \frac{\sqrt{M}-1}{\sqrt{M}} \tag{2}$$

where $\mu_c = 2\dfrac{v}{\sqrt{\pi a_{AR}}}$, v is the average velocity of an MN, $a_{AR} = \pi R^2$ and R is the access router radius.

Modeling the probability distribution of the number of boundary crossing during a call plays a significant role in cost analysis for wireless cellular networks. This will be the case again for IP-based wireless networks. Fig. 3 shows the timing diagram for typical mobile user crossing access router i (AR_i) boundary and moves to AR_j during inter-session time. t_{rs} denotes a residual subnet residence time. In case of inter-AN/MAP movement, a similar figure for timing diagram for access network boundary crossing may be drawn by replacing AR by MAP, t_c by t_d and t_{rs} by the residual access network residence time (t_{ra}).

According to the notation of Table I and the timing diagram illustration, the subnet crossing probability (P_c) and AN/MAP domain crossing probability (P_d) during inter-session time interval are expressed as follows:

$$\begin{aligned} P_c &= Pr(t_s > t_c) = \int_0^{\infty} Pr(t_s > u) f_c(u)du \\ P_d &= Pr(t_s > t_d) = \int_0^{\infty} Pr(t_s > u) f_d(u)du. \end{aligned} \tag{3}$$

The probability that an MN experiences k subnets boundary crossings and m access network boundary crossings during its session lifetime corresponds to probability mass function of N_c and N_d, respectively and expressed as follows [17]:

$$\begin{aligned} Pr(N_c = k) &= P_c^k(1-P_c) \\ Pr(N_d = m) &= P_d^m(1-P_d). \end{aligned} \tag{4}$$

TABLE I
NOTATION.

t_c	subnet (AR's coverage area) residence time random variable
t_d	AN/MAP domain residence time random variable
f_c(resp. f_d)	probability density function (PDF) of t_c (respectively t_d)
t_s	inter-session time between two consecutive sessions with PDF f_s
N_c	number of subnets crossing during intra-AN/MAP handoffs
N_d	number of AN/MAP domain crossing during inter-AN/MAP handoffs
C^g	global binding update cost to HA/CNs
C^l	local binding update cost to MAP
M	number of subnets in AN/MAP domain
N_{CN}	number of CNs having a binding cache entry for an MN
$d_{X,Y}$	average number of hops between nodes X and Y
$C_{X,Y}$	transmission cost of control packets between nodes X and Y
PC_X	processing cost of control packet at node X
C_{hc}	binding update cost at HA and CNs
C_{rr}	signaling cost for return routability procedure
t_T	time period from the L2 trigger to the starting of link switching

Then, the average number of location binding updates during an inter-session time interval under subnet crossing ($E(N_c)$) and AN/MAP domain crossing ($E(N_d)$) are given by:

$$E(N_c) = \sum_{k=0}^{\infty} kPr(N_c = k) = \sum_{k=0}^{\infty} kP_c^k(1 - P_c)$$
$$E(N_d) = \sum_{m=0}^{\infty} mPr(N_d = m) = \sum_{m=0}^{\infty} mP_d^m(1 - P_d). \tag{5}$$

For simplicity and easy derivation of signaling cost, exponential assumption is made. In other words, we assume that residence time in a subnet and in AN/MAP domain follow exponential distribution with parameters μ_c and μ_d, respectively while session arrival process follows a Poisson distribution with rate λ_s. Hence, boundary crossing probabilities and average number of location updates during an inter-session time interval can be easily obtained as follows:

$$P_c = \frac{\mu_c}{\mu_c + \lambda_s} \quad \text{and} \quad P_d = \frac{\mu_d}{\mu_d + \lambda_s}$$
$$E(N_c) = \frac{\mu_c}{\lambda_s} \quad \text{and} \quad E(N_d) = \frac{\mu_d}{\lambda_s}. \tag{6}$$

Similarly, we can derive the expression of the average number of subnets, $E(N_l)$, that an MN crosses but still stay within AN/MAP domain during an inter-session time interval.

B. Total Signaling Cost

Performance analysis of wireless networks should consider a total signaling cost induced by mobility management schemes. As for wireless cellular networks, signaling traffic overhead cost must be evaluated for NGWN or IP-based mobile environments. In NGWN, there are two kinds of location update signaling. One occurs from an MN's subnet crossing and the other occurs when the binding is about to expire. To differentiate them, the former refers to binding update (BU) message and the last one refers to binding refresh (BR) message. Moreover, delivery of data packets induces usage of network resources, then generates an additional cost. Thus, the total signaling cost, C_T, could be considered as the sum of binding update signaling cost, C_{BU}, binding refresh signaling cost, C_{BR}, and packet delivery cost, C_{PD}:

$$C_T = C_{BU} + C_{BR} + C_{PD}.$$

Since the signaling cost required for authentication and for L2 handoff are the same for all protocols; then, they are omitted in our analysis.

C. Binding Update Signaling Cost

Depending on the type of movement and the mobility management protocol, two kinds of binding updates can be performed: *local* and *global*. For MIPv6 and FMIPv6, global binding update is performed regardless of movement every time an MN acquires a new CoA and refers to registration of CoA to HA and CNs. However, for HMIPv6, global binding update occurs when an MN moves out of its MAP domain while local binding update is performed when an MN changes its current IP address within a MAP domain. Hence, the average binding update signaling cost for IPv6-based mobility management schemes during inter-session time interval depends heavily on the computation of the number of location binding updates and is given by:

$$C_{BU} = E(N_l)C^l + E(N_d)C^g. \tag{7}$$

To perform signaling overhead analysis, a performance factor called session-to-mobility ratio (SMR), which represents the relative ratio of session arrival rate to the user mobility rate, is introduced. The binding update signaling cost becomes:

$$\begin{aligned} C_{BU} &= \frac{1}{\lambda_s}\left(\mu_d C^g + \mu_l C^l\right) \\ &= \frac{1}{SMR\sqrt{M}}\left[C^g + (\sqrt{M} - 1)C^l\right]. \end{aligned} \tag{8}$$

The packet transmission cost in IP networks is proportional to the distance in hops between source and destination nodes. Furthermore, the transmission cost in a wireless link is generally larger than the transmission cost in a wired link [7]. Thus, the transmission cost of a control packet between nodes X and Y belonging to the wired part of a network can be expressed as $C_{X,Y} = \tau d_{X,Y}$ while $C_{MN,AR} = \tau\kappa$, where τ is the unit transmission cost over wired link and κ the weighting factor for the wireless link. The global and local binding update signaling costs for MIPv6 and HMIPv6 are given by:

$$C^{g}_{MIPv6} = C^{l}_{MIPv6} = 4C_{MN,AR} + 2PC_{AR} + C_{hc}$$
$$C^{l}_{HMIPv6} = 2(2C_{MN,AR} + PC_{AR} + C_{MN,MAP}) + PC_{MAP} \quad (9)$$

where C_{hc} is the binding update cost at the HA and at all active CNs while C_{rr} is the signaling cost due to return routability procedure. PC_{MAP} is divided into the mapping table lookup cost and the routing cost [7], [11].

Let consider one-way transmission cost of HoTI and CoTI messages during return routability procedure as illustrated in Fig. 1(a). An MN sends one HoTI message to its HA at a cost $C_{MN,HA}$. The HA processes this message at a cost PC_{HA} and forwards it to all CNs with $N_{CN}C_{HA,CN}$ as cost. Each CN processes the received HoTI message before to respond with HoT message, inducing a processing cost equal to $N_{CN}PC_{CN}$. Then, the cost for home address test is: $2[C_{MN,HA} + PC_{HA} + N_{CN}C_{HA,CN}] + N_{CN}PC_{CN}$. During the care-of address test, CoTI and CoT messages are exchanged directly between an MN and CNs. Then, the care-of address test cost is: $2N_{CN}C_{MN,CN} + N_{CN}PC_{CN}$. We can then deduce the expression of C_{rr} which is given in Table II.

The link layer information (L2 trigger) is used either to predict or rapidly respond to handover events in FMIPv6. Hence, signaling cost of FMIPv6 depends on the probability that handover anticipation is correct. We assume that if an MN receives FBAck message from the PAR, then it will definitely start L3 handover to NAR without exceptions. Hence, if there is no real handover after L2 trigger, all messages exchanged from RtSolPr to FBU may be unnecessary. The local binding update signaling cost for FMIPv6 is expressed as follows:

$$C^{l}_{FMIPv6} = P_s S_s + (1 - P_s)(S_f + S_r) + C_{hc} \quad (10)$$

where S_s denotes the signaling cost for a successfully anticipated handoff, S_f the signaling cost for control messages if no real L3 handoff occurs and S_r the signaling cost for reactive mode of FMIPv6. Their expressions are given in Table II.

Similar reasoning and assumption as for FMIPv6 allow computation of signaling cost for F-HMIPv6. The local binding update signaling cost of F-HMIPv6 is expressed as follows:

$$C^{l}_{FHMIPv6} = P_s S^{l}_{s} + (1 - P_s)S^{l}_{f} + S^{l}_{h}. \quad (11)$$

S^{l}_{s} and S^{l}_{f} have the same meaning as given above for FMIPv6 while S^{l}_{h} is introduced for convenient short form. Their expressions are given in Table II. FMIPv6 and HMIPv6 can enhance performance of MIPv6 for movement within AN/MAP domain. However, for inter-AN/MAP movement, performance of FMIPv6 and HMIPv6 becomes identical to that of MIPv6. If inter-MAP tunnel is not supported, the same remarks apply to F-HMIPv6.

D. Binding Refresh Cost

The binding refresh (BR) message is typically used when the cached binding is in active use but the binding's lifetime is close to expiration [2]. Usually, performance analysis available in the literature did not take into account the periodic binding refresh and the effect of a binding lifetime period. However, these parameters may have significant effect on the total signaling cost. We consider it in our performance analysis and we propose the binding refresh cost. Let T_M, T_H and T_C be the binding lifetime period for the MN at MAP, HA and CNs, respectively. The average rate of sending BR message to MAP under HMIPv6 while an MN stays in a subnet is $\lfloor 1/(\mu_c T_M) \rfloor$ where $\lfloor X \rfloor$ is the integer part of a real number X. By replacing $\mu_c T_M$ with $\mu_d T_C$ and $\mu_d T_H$, respectively, we obtain average rates of sending BR message to CN and to HA. Hence, the average binding refresh costs for HMIPv6 and F-HMIPv6 can be derived as follows:

$$C^{HMIPv6}_{BR} = 2\left(\left\lfloor \frac{1}{\mu_c T_M} \right\rfloor C_{MN,MAP} + \left\lfloor \frac{1}{\mu_d T_H} \right\rfloor C_{MN,HA}\right) + 2\left\lfloor \frac{1}{\mu_d T_C} \right\rfloor N_{CN} C_{MN,CN}. \quad (12)$$

By ignoring the binding refresh cost at MAP, we can obtain similar expression for MIPv6 and FMIPv6.

E. Packet Delivery Cost

Similarly to [19], we divide handoff latency into three components: link switching or L2 handoff latency (t_{L2}), IP connectivity latency (t_{IP}) and location update latency (t_U). IP connectivity latency reflects how quickly an MN can send IP packets after L2 handoff while location update latency is the latency of forwarding IP packets to MN's new IP address. On the other hand, the time from the starting point of L2 handoff to when an MN first receives IP packets for the first time after link switching refers to packet reception latency (t_P) or handoff latency. Moreover, we define the following delay components: movement detection delay (t_{MD}), addresses configuration and DAD procedure delay (t_{AC}), binding update latency (t_{BU}) and delay from completion of binding update and reception of first packet at the new IP address (t_{NR}).

Fig. 4 illustrates the timing diagram associated to MIPv6 and shows that there is a delay before an MN begins to receive packets directly through the NAR.

The packet delivery cost incurs during ongoing session and is composed of packet transmission and processing costs. The packet delivery cost could be defined as the linear combination of packet tunneling cost (C_{tun}) and packet loss cost (C_{loss}). Let α and β be weighting factors (where $\alpha + \beta = 1$), which emphasize tunneling effect and dropping effect; then, the packet delivery cost is computed as follows:

$$C_{PD} = \alpha C_{tun} + \beta C_{loss}. \quad (13)$$

Let s_c and s_d be the average size of control packets and data packets, respectively and $\eta = s_d/s_c$. The cost of transferring data packet is η greater than the cost of transferring control

TABLE II
EXPRESSION OF PARTIAL SIGNALING COSTS.

S_f	=	$3C_{MN,PAR} + 2C_{PAR,NAR} + 3PC_{AR}$
S_s	=	$4C_{MN,PAR} + 3C_{PAR,NAR} + 2C_{MN,NAR} + 5PC_{AR}$
S_r	=	$2C_{MN,PAR} + 2C_{PAR,NAR} + 2C_{MN,NAR} + 3PC_{AR}$
S_f^l	=	$3C_{MN,MAP} + 2(C_{MAP,NAR} + PC_{MAP}) + PC_{AR}$
S_s^l	=	$4C_{MN,MAP} + 3C_{MAP,NAR} + 2C_{MN,NAR} + 3PC_{MAP} + 2PC_{AR}$
S_h^l	=	$P_s[2(C_{MN,NAR}+C_{NAR,MAP})+PC_{NAR}+PC_{MAP}]+(1-P_s)C_{HMIPv6}^l$
C_{hc}	=	$2(C_{MN,HA} + N_{CN}C_{MN,CN}) + PC_{HA} + N_{CN}PC_{CN} + C_{rr}$
C_{rr}	=	$2(C_{MN,HA} + N_{CN}C_{HA,CN} + N_{CN}C_{MN,CN} + PC_{HA} + N_{CN}PC_{CN})$

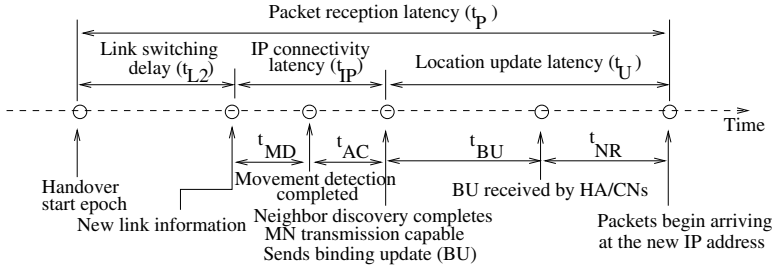

Fig. 4. Handoff delay timeline of MIPv6.

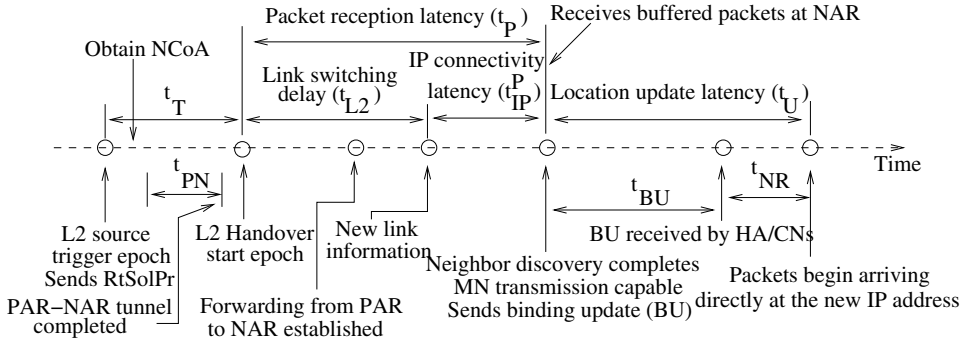

Fig. 5. Handoff delay timeline of FMIPv6.

packet. Let λ_p be the packet arrival rate in unit of packet per time. There is no forwarding with MIPv6 during handover (i.e., $C_{tun}^{MIPv6} = 0$); then, only packet loss cost occurs and is evaluated as follows:

$$C_{loss}^{MIPv6} = \lambda_p C_{cm}^{f,1}(t_{L2} + t_{IP} + t_U) \tag{14}$$

where $C_{cm}^{f,1} = \eta(C_{CN,PAR} + C_{PAR,MN})$ is the cost of transferring data packets from CN to MN via PAR when the handoff fails, $t_U = t_{BU} + t_{NR}$, $t_{BU} = t_{HA} + t_{RR} + t_{CN}$ with t_{HA} is the delay for performing BU procedure to the HA, t_{RR} is the delay for return routability procedure and t_{CN} is the delay for performing BU process to all active CNs.

In HMIPv6, all packets directed to MN will be received by MAP and after being tunneled to MN's current address (LCoA) by using mapping table. Then, the lookup time of mapping table has an effect on MAP's processing cost. Similarly to MIPv6, there is no forwarding with HMIPv6 during handover (i.e., $C_{tun}^{HMIPv6} = 0$). Hence, packet delivery cost for intra-AN/MAP roaming can be computed through (13), where packet loss cost, C_{loss}^{HMIPv6}, is given by:

$$C_{loss}^{HMIPv6} = \lambda_p C_{cm}^{f,2}(t_{L2} + t_{IP} + t_U^L) \tag{15}$$

where t_U^L is the location update latency for intra-AN/MAP roaming: $t_U^L = t_{BU}^L + t_{NR}^L$ with t_{BU}^L the local binding update latency at MAP while t_{NR}^L is equivalent to t_{NR} for local roaming and the transferring data packets cost between CN and MN when the handoff fails is

$$C_{cm}^{f,2} = \eta(C_{CN,MAP} + C_{MAP,PAR} + C_{PAR,MN} + PC_{MAP}).$$

To avoid packet loss, FMIPv6 enables PAR to forward packets to NAR by using a bi-directional tunnel established between them and by buffering all forwarded packets. The timing diagram of predictive mode of FMIPv6 is shown in Fig. 5 and the packet tunneling cost is given by:

$$C_{tun}^{FMIPv6,p} = \lambda_p C_{cm}^{s,1}(t_{L2} + t_{IP}^P + t_U) \tag{16}$$

where $C_{cm}^{s,1} = \eta(C_{CN,PAR} + C_{PAR,NAR} + C_{NAR,MN})$ is the cost of transferring data packets from CN to MN by transiting to PAR and forwarding to NAR via the established tunnel, and

t_{IP}^{P} is the IP connectivity latency for predictive mode of fast handover scheme, $t_{IP}^{P} \leq t_{IP}$.

The packet loss due to L2 handoff delay is inevitable without an efficient buffering mechanism. Moreover, packet loss in FMIPv6 may be due to wrong temporal and spatial predictions. Let t_{PN}, the time required to establish a tunnel between PAR and NAR. Usually, t_T is greater than t_{PN}; then, packets received during handover procedure are forwarded by PAR to NAR by using the already established tunnel. But, if MN moves very fast, t_T may be less than t_{PN}. Then, packets arriving to PAR during the time period $t_{PN} - t_T$ may be lost, because the tunnel is not yet established. In other words, for the anticipated signaling to succeed, the following time constraint must be observed: $t_{PN} \leq t_T$. Hence, packet loss cost for predictive mode of FMIPv6 can be expressed as follows:

$$C_{loss}^{FMIPv6,p} = \lambda_p C_{cm}^{f,1} \max(t_{PN} - t_T, 0). \tag{17}$$

Due to wrong spatial prediction of NAR or if FBAck message was not received on the previous link, the forwarded packets by PAR may be lost. In this case, the reactive mode of FMIPv6 is used. Let t_{IP}^{R}, the IP connectivity latency of reactive mode. Since the packets forwarding process is not supported in the reactive mode; then, packet tunneling cost is equal to zero while packet loss cost for reactive mode of FMIPv6 can be expressed as follows:

$$C_{loss}^{FMIPv6,r} = \lambda_p C_{cm}^{f,1}(t_{L2} + t_{IP}^{R} + t_U). \tag{18}$$

Hence, the average packet delivery cost of FMIPv6 in terms of prediction accuracy is given by:

$$C_{PD}^{FMIPv6,a} = P_s C_{PD}^{FMIPv6,p} + (1 - P_s) C_{PD}^{FMIPv6,r}. \tag{19}$$

With reasoning similar to FMIPv6, evaluation of packet delivery cost for intra-AN/MAP roaming for F-HMIPv6 is obtained by replacing t_U, t_{PN}, t_{IP}^{R}, $C_{cm}^{s,1}$ and $C_{cm}^{f,1}$, respectively by t_U^L, t_{ML}, t_{IP}, $C_{cm}^{s,2}$ and $C_{cm}^{f,2}$. Where $C_{cm}^{s,2}$ is the cost of transferring data packets from CN to MN by transiting through the MAP and NAR given by

$$C_{cm}^{s,2} = \eta(C_{CN,MAP} + C_{MAP,NAR} + C_{NAR,MN} + PC_{MAP})$$

and t_{ML} is the time required to establish a tunnel between MAP and NAR. For inter-AN/MAP roaming, the packet delivery cost of HMIPv6, FMIPv6 and F-HMIPv6 becomes the same as for MIPv6.

F. Required Buffer Space

In FMIPv6, NAR buffers packets tunneled from PAR and forwards them to MN when the latter announces its presence on the new link. Hence, the required buffer space during MN's subnet movement increases in proportion of the packet arrival rate and according to the number of MNs performing handover. The buffer space required for FMIPv6 during intra-AN/MAP handover is proportional to handoff latency and is computed as follows:

$$BS_{FMIPv6}^{l} = \lambda_p[P_s(t_{L2} + t_{IP}^{P} + t_U) + (1 - P_s)t_{NR}]. \tag{20}$$

Similarly, buffer space required for F-HMIPv6 is obtained by replacing t_U and t_{NR} by t_U^L and t_{NR}^L in (20), respectively. Since MIPv6 and HMIPv6 do not use handover anticipation techniques; then, by setting $P_s = 0$ in (20), we obtain a required buffer space for MIPv6 and HMIPv6.

G. Handoff Latency and Packet Loss

We define the following parameters to compute handoff latency and packet loss: t_{L2} the L2 handoff latency, t_{RD} the round-trip time for router discovery procedure, t_{DAD} the time for DAD process execution, t_{RR} the delay for an MN to perform return routability procedure and $t_{X,Y}$ one-way transmission delay of a message of size s between nodes X and Y. Since the average delay needed for an MN authentication is the same for all protocols; then, it is omitted. If one of the endpoints is an MN, $t_{X,Y}$ is computed as follows:

$$t_{X,Y}(s) = \frac{1-q}{1+q}\left(\frac{s}{B_{wl}} + L_{wl}\right) + (d_{X,Y} - 1)\left(\frac{s}{B_w} + L_w + \varpi_q\right) \tag{21}$$

where q is the probability of wireless link failure, ϖ_q the average queueing delay at each router in the Internet [20], B_{wl} (resp. B_w) the bandwidth of wireless (resp. wired) link and L_{wl} (resp. L_w) wireless (resp. wired) link delay. The handoff latency associated to MIPv6 is given by:

$$D_{MIPv6} = t_{L2} + t_{RD} + t_{DAD} + t_{RR} + 2(t_{MN,HA} + t_{MN,CN}). \tag{22}$$

The handoff latency for intra-AN/MAP or localized movement of HMIPv6 is obtained by replacing HA by MAP and by ignoring t_{RR} and $t_{MN,CN}$ in (22). Let Δ_{ns} be the time elapsed from the reception of FBAck on previous link to the beginning of L2 handoff when there is no good synchronization between L2 and L3 handoff mechanisms. Moreover, let Δ_{lr} be the time between last packet reception through previous link and L2 handoff beginning when FBAck is received on new link. Note that, Δ_{lr} and Δ_{ns} may be equal to zero and we use this assumption in performance analysis. For fast handoff schemes, the handoff latency depends on information availability, and on which link fast handoff messages are exchanged. Hence, if information about NAR and impending handoff are available, and FBAck message is received through the previous link, handoff latency for localized or micro-mobility without an efficient buffers management for FMIPv6 and F-HMIPv6 is expressed as follows:

$$O_{FMIPv6}^{l} = O_{FHMIPv6}^{l} = \Delta_{ns} + t_{L2} + 2t_{MN,NAR}. \tag{23}$$

If FBAck message is not received through previous link, F-HMIPv6 turns to HMIPv6 while for FMIPv6 its reactive mode is used. Then, handoff latency without efficient buffer management for FMIPv6 is expressed as follows:

$$N_{FMIPv6}^{l} = \Delta_{lr} + t_{L2} + 2t_{MN,NAR} + 3t_{NAR,PAR}. \tag{24}$$

The average handoff latency for FMIPv6 in terms of prediction probability is given by:

$$D_{FMIPv6}^{l} = P_s O_{FMIPv6}^{l} + (1 - P_s) N_{FMIPv6}^{l}. \tag{25}$$

Similarly, we can obtain the average handoff latency for F-HMIPv6. The predictive mode of FMIPv6 cannot perform

TABLE III
SYSTEM PARAMETERS.

Parameters	Symbols	Values
DAD delay	t_{DAD}	500 ms
Router discovery delay	t_{RD}	100 ms
L2 handoff delay	t_{L2}	50 ms
Prediction probability	P_s	0.90
Wireless link failure probability	q	0.50
Wired link bandwidth	B_w	100 Mbps
Wireless link bandwidth	B_{wl}	11 Mbps
Wired link delay	L_w	2 ms
Wireless link delay	L_{wl}	10 ms
Number of ARs by AN/MAP	M	2
Control packet size	s_c	96 bytes
Data packet size	s_d	200 bytes
Packet arrival rate	λ_p	10 packets/s
MN average speed	v	5.6 Km/h
Subnet radius	R	500 m

anticipated IP-handoff for inter-AN [6]; then handoff latency of FMIPv6 becomes same as for MIPv6. The same remark applies to HMIPv6 and F-HMIPv6.

With MIPv6 and HMIPv6, packet loss occurs during handoff latency or service disruption latency. In fact, the number of packet loss is proportional to handoff latency. This is also the case for FMIPv6 and F-HMIPv6 if there is no efficient buffer management (BM). In fact, for fast handoff schemes there is no packet loss in theory, unless buffer overflow happens. Hence, the number of packet lost for each handoff management scheme is computed as follows:

$$P_{loss}^{scheme,l} = \begin{cases} \max(BS_{scheme}^{l} - B, 0) & \text{for efficient BM} \\ \lambda_p D_{scheme}^{l} & \text{otherwise} \end{cases} \quad (26)$$

where B is the buffer size of an AR and BS_{scheme}^{l} is the buffer space required at an access router for a given scheme (i.e., MIPv6, HMIPv6, FMIPv6 or F-HMIPv6).

IV. PERFORMANCE EVALUATION

Parameters and default values used in performance evaluation are given in Table III, except when wireless link delay and packet arrival rate are considered as variable parameters. The network topology considered for analysis is illustrated in Fig. 6, where ER means edge router. For protocols which do not involve hierarchical mobility management, the MAPs act as a normal intermediate (edge) router. We assume that distance (i.e., the number of hops) between different domains are equals, i.e., $c = d = e = f = 10$ and we set $a = 1$, $b = 2$. The time-to-live (TTL) field in IP packet headers may be used by an MN to get the number of hops packets travel. Then, this distance varies within a certain range [7]. All links are supposed to be full-duplex in terms of capacity and delay. Other parameters used for cost computation are defined as follows: $\tau = 1$, $\kappa = 10$, $\alpha = 0.2$, $\beta = 0.8$, $\sigma = 2$, $PC_{AR} = 8$, $PC_{HA} = 24$, $PC_{CN} = 4$ and $PC_{MAP} = 12$.

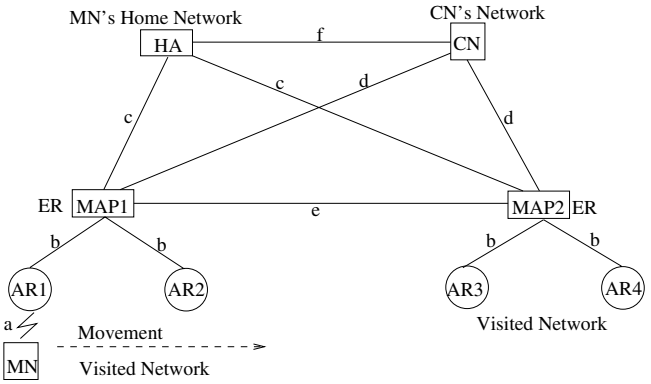

Fig. 6. Network topology used for analysis.

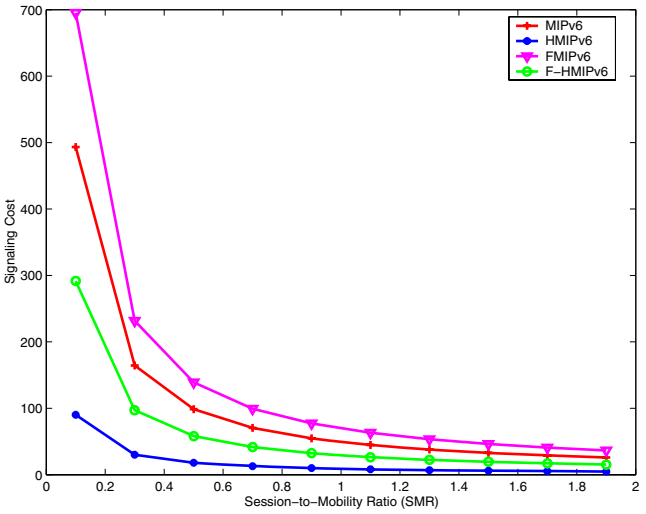

Fig. 7. Impact of session-to-mobility ratio on binding update signaling cost.

Most parameters used in this analysis are set to typical values found in [7], [10], [21].

Fig.7 illustrates the binding update signaling cost during handoff as a function of SMR for intra-AN/MAP roaming. When SMR is small, the mobility rate is larger than session arrival rate; then, an MN changes subnet frequently due to its mobility, inducing several handoffs and the signaling overhead increases. However, when the session arrival rate is larger than mobility rate (i.e., SMR is greater than 1), binding update is less often performed and signaling overhead decreases because the frequency of subnet changes decreases. FMIPv6 and F-HMIPv6 do not effectively reduce signaling overhead comparatively to MIPv6 and HMIPv6, respectively due to messages introduced for handoff anticipation. However, signaling overhead of fast handoff schemes is traded off by lower handoff latency and packet loss as we will see later.

Fig. 8 represents the effect of binding lifetime period on the binding refresh cost and shows that the binding refresh cost decreases as binding lifetime period increases. We assume that the binding lifetime periods T_M, T_H and T_C are equals. We can see that the binding lifetime period has significant impact on the average binding refresh cost. Small value of binding lifetime period leads to larger binding refresh cost; in other words, significant signaling load throughout the network. On

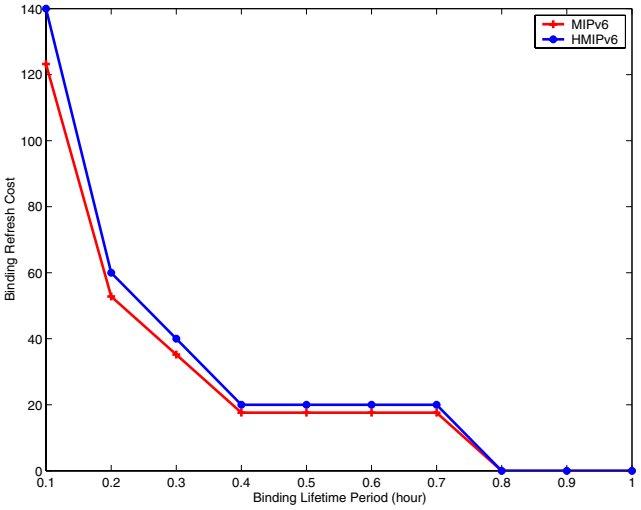

Fig. 8. Impact of binding lifetime period on binding refresh cost.

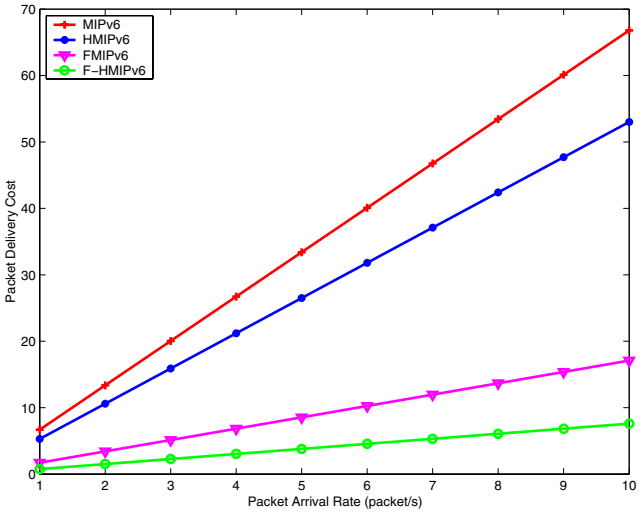

Fig. 9. Packet delivery cost as a function of packet arrival rate.

the other hand, larger value of the binding lifetime period leads to larger binding cache entry at mobility agents. This may result in higher memory consumption and higher binding cache lookup time.

The result shows that the binding refresh cost remains constant when the binding lifetime period is between 0.4 and 0.7 hour and as well as when it is greater than 0.8 hour. For the former case, the result indicates that during $[0.4, 0.7]$ time period there is the same number of binding refresh messages. This is due to the fact that an MN moves to an adjacent subnet before the new binding refresh message occurs. While for the latter case, the average subnet residence time of an MN is shorter than the binding lifetime period (i.e., $T_M \geq 0.8$ hour). Hence, no binding refresh message occurs and the binding refresh cost is equal to zero. On the other hand, due to binding cache and lookup table maintained at the MAP, there is an extra cost for binding refresh process at the MAP for HMIPv6. Thus, binding refresh cost of HMIPv6 is slightly greater than for MIPv6.

The packet delivery cost is depicted in Fig. 9 as a function of packet arrival rate (λ_p). We observe that, packet delivery cost increases proportionally with λ_p for all schemes. Fast handoff schemes (i.e., F-HMIPv6 and FMIPv6) outperform MIPv6 and HMIPv6, and they are more efficient when λ_p increases. This means that FMIPv6 and F-HMIPv6 are better suited for real-time applications where periodic packets are sent at high rates. The packet delivery cost depends on handoff latency, while packet loss is proportional to handoff latency. Then, a similar analysis may be performed for packet loss when comparing to packet arrival rate as in Fig. 9. Hence, packet loss will be lesser for fast handoff schemes than for MIPv6 and HMIPv6.

For varying prediction probability, P_s, Fig. 10 shows the behavior of packet delivery cost. The packet delivery cost decreases when the accuracy of P_s increases for fast handoff schemes. Due to additional packet processing at MAP for F-HMIPv6, there is an extra cost for packet delivery with inaccuracy prediction. In fact, in this case, F-HMIPv6 turns to HMIPv6, as we can see when $P_s = 0$. HMIPv6 and MIPv6

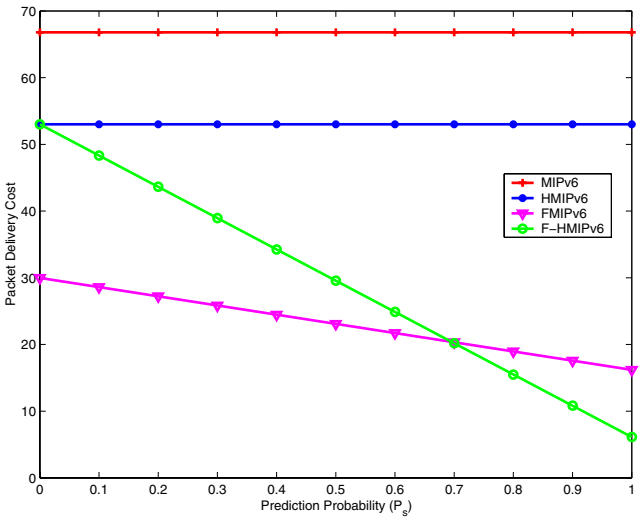

Fig. 10. Packet delivery cost as a function of prediction probability.

are not affected by the prediction probability. For high values of P_s, F-HMIPv6 performs better than FMIPv6. Since there is a relation between handoff latency and packet delivery cost, a similar behavior will be observed when comparing handoff latency with prediction probability. Hence, an effective prediction mechanism is required to allow better performance for F-HMIPv6.

To alleviate packet losses, fast handover schemes should support packet buffering and forwarding during handoff execution. Since fast handover schemes start packet buffering and forwarding earlier; then, they require more buffer space than MIPv6 and HMIPv6 as we can see in Fig. 11. On the other hand, buffering time may affect real-time applications, for example if some packets are stored in a buffer for a longer period of time than acceptable end-to-end delay, they may become useless. Hence, it is crucial to manage buffers efficiently in order to minimize overhead and to provide better QoS to delay sensitive applications.

In Fig. 12, we can see that the handover latency increases proportionally with the wireless link delay. We observe that

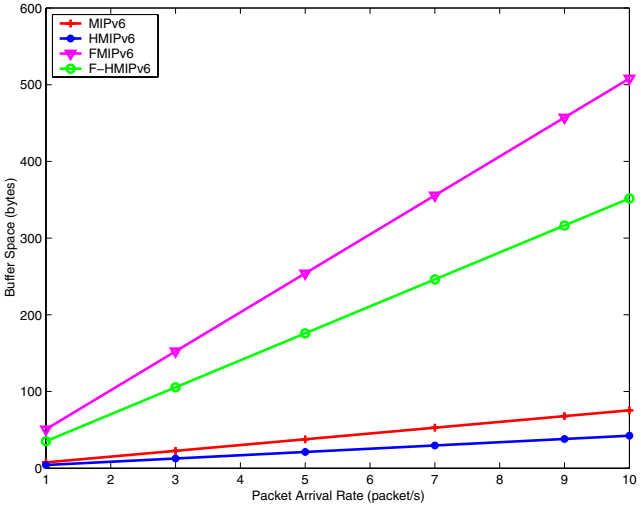

Fig. 11. Required buffer space as a function of packet arrival rate.

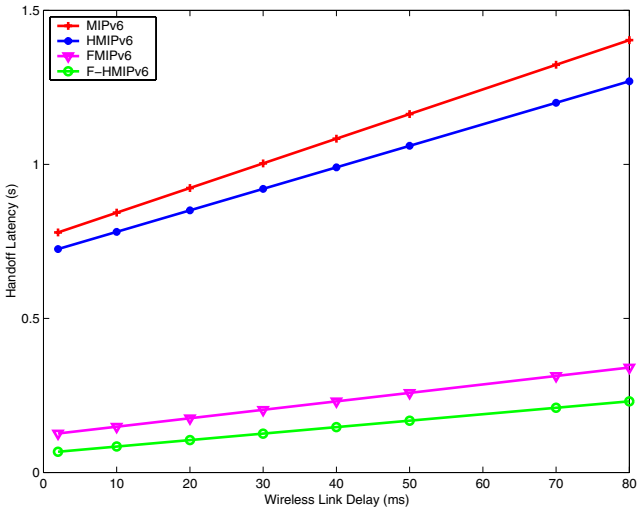

Fig. 12. Impact of wireless link delay on handoff latency.

MIPv6 and HMIPv6 have worst results among all protocols followed by FMIPv6 while F-HMIPv6 performs better than all other schemes. For MIPv6 and HMIPv6, the DAD process counts for a large portion of handoff delay. Therefore, it is important to decrease the DAD delay in order to decrease handoff latency. The optimistic DAD (oDAD) [22] has recently been proposed to allow minimization of address configuration delay by eliminating the DAD completion time.

V. Conclusion

Mobility management is a key issue in next-generation or 4G wireless networks (NGWN/4G). Several IPv6-based mobility schemes have been proposed in the literature and by IETF. However, they are not able to guarantee seamless roaming and service continuity for critical applications like real-time applications. Moreover, performance evaluation of these schemes is usually based on simulation approaches.

This paper proposes a comprehensive analytical model for IPv6-based mobility protocols (i.e., MIPv6, HMIPv6, FMIPv6 and F-HMIPv6) in order to provide depth analysis of the overall performance of these protocols. Several performance metrics such as signaling overhead cost, packet delivery cost, handoff latency and packet loss are analyzed according to user mobility and traffic models. Our goal was not to decide which scheme is always better, but to study the effect of various parameters related to mobility and traffic on the performance of these schemes in order to facilitate decision-making for wireless network design.

The numerical results show the potential pros and cons of most promising IPv6-based mobility schemes proposed by IETF. They reveal that F-HMIPv6 enables improvement in terms of handoff latency and packet loss rather than other protocols (i.e., MIPv6, HMIPv6 and FMIPv6). However, this performance is off-set by its signaling traffic overhead and the buffer space required when compared to HMIPv6. Moreover, it is very difficult to forecast which IPv6-based mobility protocol will dominate in NGWN/4G. In fact, selection of a mobility management scheme is not based solely on performance criteria, but on cost and respective profits as well. Thus, until an ideal mobility management protocol is designed and deployed, mobile users still require a practical solution. This could be achieved by a certain tradeoff of the above requirements.

Acknowledgment

The authors would like to thank the anonymous reviewers for their helpful feedback, suggestions and comments to improve the presentation of this paper.

References

[1] I. F. Akyildiz, S. Mohanty, and J. Xie, "A ubiquitous mobile communication architecture for next-generation heterogeneous wireless systems," *IEEE Commun. Mag.*, vol. 43, no. 6, pp. 29-36, June 2005.

[2] D. B. Johnson, C. E. Perkins, and J. Arkko, "Mobility support in IPv6," IEFT RFC 3775, June 2004.

[3] G. Koodli, "Fast handovers for mobile IPv6," IETF RFC 4068, July 2005.

[4] H. Soliman, C. Castelluccia, K. El-Malki, and L. Bellier, "Hierarchical mobile IPv6 mobility management (HMIPv6)," IETF RFC 4140, Aug. 2005.

[5] X. Pérez-Costa, M. Torrent-Moreno, and H. Hartenstein, "A performance comparison of mobile IPv6, hierarchical mobile IPv6, fast handovers for mobile IPv6 and their combination," *ACM Mobile Computing and Commun. Rev.*, vol. 7, no. 4, pp. 5-19, Oct. 2003.

[6] Y. Gwon, J. Kempf, and A. Yegin, "Scalability and robustness analysis of mobile IPv6, fast mobile IPv6, hierarchical mobile IPv6, and hybrid IPv6 mobility protocols using a large-scale simulation," in *Proc. IEEE Int. Conf. on Commun.* (ICC'04), vol. 7, June 2004, pp. 4087-4091.

[7] J. Xie and I. F. Akyildiz, "A novel distributed dynamic location management scheme for minimizing signaling costs in mobile IP," *IEEE Trans. Mobile Computing*, vol. 1, no. 3, pp. 163-175, July/Sept. 2002.

[8] X. Pérez-Costa, R. Schmitz, H. Hartenstein, and M. Leibsch, "A MIPv6, FMIPv6 and HMIPv6 handover latency study: analytical approach," in *Proc. IST Mobile and Wireless Commun. Summit*, June 2002, pp. 100-105.

[9] C. Castelluccia, "HMIPv6: a hierarchical mobile IPv6 proposal," *ACM Mobile Computing and Commun. Rev.*, vol. 4, no. 1, pp. 48-59, Jan. 2000.

[10] S. Pack and Y. Choi, "Performance analysis of fast handover in mobile IPv6 networks," in *Proc. IFIP Pers. Wireless Commun.*, LNCS, vol. 2775, Sept. 2003, pp. 679-691.

[11] S. Pack and Y. Choi, "A study on performance of hierarchical mobile IPv6 in IP-based cellular networks," *IEICE Trans. Commun.*, vol. E87-B, no. 3, pp. 462-469, March 2004.

[12] S. Thomson and T. Narten, "IPv6 stateless address autoconfiguration," IETF RFC 2462, Dec. 1998.

[13] K. D. Wong, A. Dutta, H. Schulzrinne, and K. Young, "Simultaneous mobility: analytical framework, theorems and solutions," *Wireless Commun. and Mobile Computing* (Wiley), to appear.

[14] H. Y. Jung, E. A. Kim, J. W. Yi, and H. H. Lee, "A scheme for supporting fast handover in hierarchical mobile IPv6 networks," *ETRI Journal*, vol. 27, no. 6, pp. 798-801, Dec. 2005.
[15] W. Wang and I. F. Akyildiz, "Intersystem location update and paging schemes for multitier wireless networks," in *Proc. ACM MOBICOM*, Aug. 2000, pp. 99-109.
[16] F. V. Baumann and I. G. Niemegeers, "An evaluation of location management procedures," in *Proc. 3rd Annual Int. Conf. Universal Personal Commun.* (UPC'94), Sept./Oct. 1994, pp. 359-364.
[17] Y. Xiao, Y. Pan, and J. Lie, "Design and analysis of location management for 3G cellular networks," *IEEE Trans. Parallel Distrib. Syst.*, vol. 15, no. 4, pp. 339-349, April 2004.
[18] Y. Fang, "Movement-based mobility management and trade off analysis for wireless mobile networks," *IEEE Trans. Computers*, vol. 52, no. 6, pp. 791-803, June 2003.
[19] R. Koodli and C. E. Perkins, "Fast handovers and context transfers in mobile networks," *ACM Mobile Computing and Commun. Rev.*, vol. 31, no. 5, Oct. 2001.
[20] J. McNair, I. F. Akyildiz, and M. D. Bender, "Handoffs for real-time traffic in mobile IP version 6 networks," in *Proc. IEEE GLOBECOM*, vol. 6, Nov. 2001, pp. 3463-3467.
[21] W. K. Lai and J. C. Chiu, "Improving handoff performance in wireless overlay networks by switching between two-layer IPv6 and one-layer IPv6 addressing," *IEEE J. Select. Areas Commun.*, vol. 23, no. 11, pp. 2129-2137, Nov. 2005.
[22] N. Moore, "Optimistic duplicate address detection," IETF RFC 4429, April 2006.

Christian Makaya (S'06) received the M.Sc. degrees in Computer Science from University of Montreal (2003) and in Telecommunications (2004) from INRS-EMT, University of Quebec, Montreal, Canada. He is currently pursuing a Ph.D. in Computer Engineering (thesis carried out jointly with Ericsson Research Canada) at the Ecole Polytechnique de Montreal, Montreal, Canada, while working as a Graduate Research Assistant with the Mobile Computing and Networking Research Laboratory (LARIM). The current focus of his research interests is on radio resource management, interworking architectures design, mobility management, IP mobility, performance evaluation and quality of service (QoS) provisioning for next-generation wireless networks.

Samuel Pierre (SM'97) received the B.Eng. degree in Civil Engineering in 1981 from Ecole Polytechnique de Montreal, Québec, Canada, the B.Sc. and M.Sc. degrees in Mathematics and Computer Science in 1984 and 1985, respectively, from the UQAM, Montreal, the M.Sc. degree in Economics in 1987 from the University of Montreal, and the Ph.D. degree in Electrical Engineering in 1991 from Ecole Polytechnique de Montreal. From 1987 to 1998, he was a Professor at the University of Québec at Trois-Rivières prior to joining the Télé-Université of Québec, an Adjunct Professor at Université Laval, Ste-Foy, Québec, an Invited Professor at the Swiss Federal Institute of Technology, Lausanne, Switzerland, and the the Université Paris 7, France. He is currently a Professor of Computer Engineering at Ecole Polytechnique de Montreal, where he is Director of the Mobile Computing and Networking Research Laboratory (LARIM), Chairholder of the NSERC/Ericsson Chair in Next Generations and Mobile Networking Systems, and the Director of the Mobile Computing and Networking Research Group (GRIM). His research interests include wireline and wireless networks, mobile computing, artificial intelligence, and telelearning. Dr. Pierre is a Fellow of the Engineering Institute of Canada (EIC). He is a Regional Editor of the *Journal of Computer Science*, an Associate Editor of *IEEE Communications Letters*, *IEEE Canadian Journal of Electrical and Computer Engineering* and *IEEE Canadian Review*, and serves on the editorial board of *Telematics and Informatics*, edited by Elsevier Science.